



World Scientific News

An International Scientific Journal

WSN 214 (2026) 11-29

EISSN 2392-2192

Kinetics, Equilibrium and pH Effects of Atrazine Sorption on Activated Charcoal and Kaolin

Emmanuel Onyenweife Ayadinuno

Department of Pure and Industrial Chemistry, Nnamdi Azikiwe University, Awka

Author's Email: emmaonyenweife@gmail.com

<https://doi.org/10.65770/FCWW7326>

ABSTRACT

This study examined the effect of pH and the kinetics of adsorption and desorption of atrazine, an herbicide whose environmental behaviour is governed by sorption–desorption processes at solid–liquid interfaces, on activated charcoal, kaolin, and their composites. Batch experiments were conducted over pH 5–8, and time-dependent concentration changes were measured at pH 5 to model kinetic behaviour. Atrazine adsorption was essentially independent of pH in the range 5–8, consistent with its predominantly neutral speciation above pH 5. Under these conditions, electrostatic attraction between charged species is unlikely; adsorption is instead attributed mainly to van der Waals forces, hydrophobic interactions, and weak hydrogen bonding between atrazine functional groups and hydroxyl-rich surfaces. Adsorption kinetic data were fitted to zero-, first- and second-order models. Second-order plots did not obey linearity, and zero-order fits were generally poor. First-order treatment of the data produced saturation-type plots consistent with Langmuir monolayer adsorption, with equilibrium achieved in about 50 minutes on all surfaces. First-order rate constants ranged from 0.077 to 0.090 day⁻¹, corresponding to half-lives of 7.70–9.00 days, and composite matrices did not significantly enhance adsorption relative to the pure materials. Desorption, initiated after sorption equilibrium, was also analysed using zero-, first- and second-order models. Zero-order plots showed reasonable linearity, but first-order analysis again yielded saturation behaviour with clear approach to equilibrium. Desorption rate constants were 0.017–0.052 day⁻¹ with half-lives of 34.65–46.20 days. Overall, in the environmentally relevant pH window, atrazine sorption and desorption on these adsorbents are dominated by non-electrostatic interactions and are well described by first-order, Langmuir-type kinetics.

Keywords: Order, Reaction, Thermodynamics, Equilibrium, Sorption.

(Received 8 February 2026; Accepted 19 March 2026; Date of Publication 4 April 2026)

1. INTRODUCTION

Atrazine, a widely used triazine herbicide, is applied for pre- and post-emergence weed control in maize and other crops and is commonly detected in surface and groundwater due to its moderate persistence and high mobility in soils (Prasanta Majee *et al.*, 2023). Its continued occurrence in drinking water sources has raised environmental and public health concerns, prompting stringent regulatory limits in many regions and stimulating research on cost-effective removal technologies. Among the various techniques, sorption onto carbonaceous materials and clay minerals is regarded as a practical and economical option for atrazine attenuation in aqueous and soil–water systems (Prasanta Majee *et al.*, 2023).

Activated carbon–based sorbents, including powdered or granular carbons, activated carbon cloths, and biochar-derived activated carbons, have shown high atrazine uptake due to their large surface area, developed porosity, and surface functional groups (Cleuciane Tillvitz do Nascimento *et al.*, 2022, Javier M. Gonzalez *et al.*, 2020, Yamil L. Salomón *et al.*, 2022). Equilibrium data for atrazine on activated carbons are typically well described by Langmuir or Freundlich isotherms, indicating favorable sorption and, in many cases, high sorbent–sorbate affinity (Cleuciane Tillvitz do Nascimento *et al.*, 2022, Javier M. Gonzalez *et al.*; 2020). Kinetic studies commonly report rapid initial uptake followed by a slower approach to equilibrium, with pseudo-second-order and intraparticle-diffusion models frequently providing good fits and suggesting contributions from both film diffusion and pore diffusion mechanisms (Cleuciane Tillvitz do Nascimento *et al.*, 2022, Javier M. Gonzalez *et al.*, 2020). These findings underline the potential of activated carbon and related materials as key components of pollution-control structures and water-treatment systems targeting atrazine (Javier M. Gonzalez *et al.*, 2020).

Clay minerals and kaolinite-based materials also play an important role in controlling the fate of atrazine in the environment. Sorption of atrazine on soils and clay fractions is strongly influenced by mineralogy, organic matter content, surface area, and solution chemistry, particularly pH (Sun Jing *et al.*, 2020, Prasanta Majee *et al.*, 2023). Several studies have shown that lower pH conditions enhance atrazine sorption, attributed to increased protonation of the weakly basic atrazine molecule and stronger electrostatic or specific interactions with mineral and organic surfaces (Sun Jing *et al.*, 2020, Prasanta Majee *et al.*, 2023). Kaolinite and modified kaolinite clays have been identified as promising low-cost adsorbents for triazine removal, with equilibrium often described by the Langmuir isotherm and kinetics by pseudo-second-order models, indicating monolayer sorption with chemico-physical controls (Sun Jing *et al.*, 2020)

Despite extensive work on atrazine sorption onto soils, biochars, and various activated carbons, comparative studies that systematically evaluate kinetics, equilibrium behavior, and pH effects on atrazine sorption using both activated charcoal and kaolin under identical conditions remain limited (Sun Jing *et al.*, 2020, Prasanta Majee *et al.*, 2023). Such information is crucial for understanding the relative contributions of carbonaceous and clay phases to atrazine attenuation, optimizing treatment media for water purification, and improving predictive models of herbicide transport in the soil–water environment. This study, therefore, investigates the kinetics, equilibrium isotherms, and pH dependence of atrazine sorption onto activated charcoal and kaolin, with the aim of elucidating the controlling mechanisms and assessing their suitability as sorbents for atrazine removal from contaminated waters.

2. MATERIALS AND METHODS

Equipment

The following equipment was used in this research: analytical balance (Mettler Toledo); mechanical shaker (Science Laboratory Supplier, UK), centrifuge (Megafuge, Heraeus), sonicator (Fischer Scientific FB/4032), vortex mixer (Vortex Genie 2 Scientific Industries), UV-Visible spectrophotometer (Varian), pH meter (Meterlab TM PHM 290 pH-stat with a Radiometer), syringe; leaching tube; capped glass vial; and water bath.

Materials

The following materials were obtained as analytical grade from Zayo Sigma, Jos, Nigeria, and were used as received: atrazine, anhydrous citric acid, ethylamine, chloroform, sodium alginate, potassium dihydrogen phosphate (KH_2PO_4), while calcium chloride, ethanol, distilled water, kaolin, and activated charcoal were obtained from NAFDAC Zonal Laboratory, Agulu.

Preparation of Buffer Solutions

Solutions of potassium dihydrogen phosphate (KH_2PO_4) buffer were utilized in this study. A litre of 0.1M KH_2PO_4 buffer pH 4.38 was made by weighing 6.80g (0.1mol) KH_2PO_4 into 500ml water in a 1-litre volumetric flask. This was agitated with a vortex mixer to make it dissolve. Aliquots of 18 ml, 22 ml, and 26.5 ml of 1M NaOH were added into the volumetric flask to adjust the pH to 5.0, 6.0 and 8.0, respectively. These pHs were chosen to give room for cross-system comparison as most other works on atrazine were done within the same pH range. A pH meter was used to confirm the pH.

Preparation of Atrazine Stock Solutions

Stock solution of atrazine (3.50 mg/ml) was prepared by dissolving 70.00 mg of atrazine in 20 ml ethanol in a volumetric flask in order to aid solubility of the herbicide in water. Serial dilution (equ.3.1) using 1000 μL Eppendorf pipettes was carried out by measuring 1.43 ml, 2.86 ml, 3.57 ml, 4.29 ml and 5.71 ml of the stock solution into 25 ml volumetric flasks and making up to the mark using ethanol. These produced the following concentrations of atrazine, respectively: 0.20, 0.40, 0.50, 0.60, 0.80.

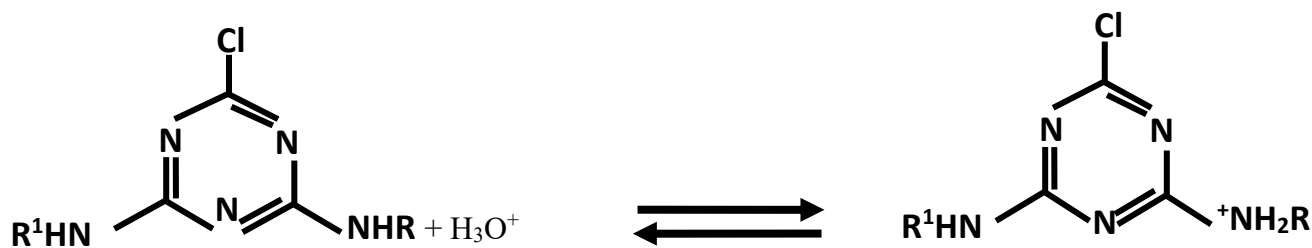
$$C_1V_1 = C_2V_2$$

1

Kinetic Experiments

In each kinetic experiment, 200 mg of the sorbent (i.e. C100, K100 KC7030, KC5050 and KC3070) was weighed into capped glass vials, and 2 ml distilled water added, followed by 3 ml buffer (pH 5, 6 or 8) and 5 ml standard herbicide solution. These were placed on the shaker. One vial each was taken at intervals of 20, 40, 60, 80, 100, 120 minutes, centrifuged at 4000rpm and 3ml of the supernatant withdrawn for spectrophotometric herbicide analysis.

3. RESULTS /EXPERIMENTAL



Scheme 1. Protonation of atrazine in acidic medium.

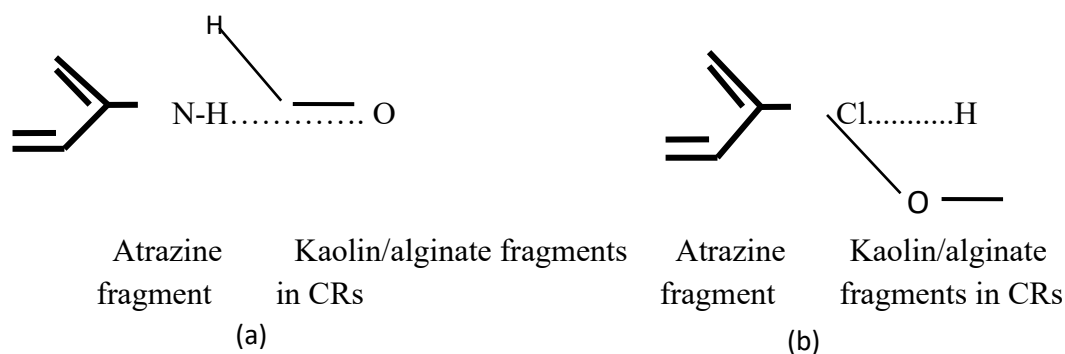
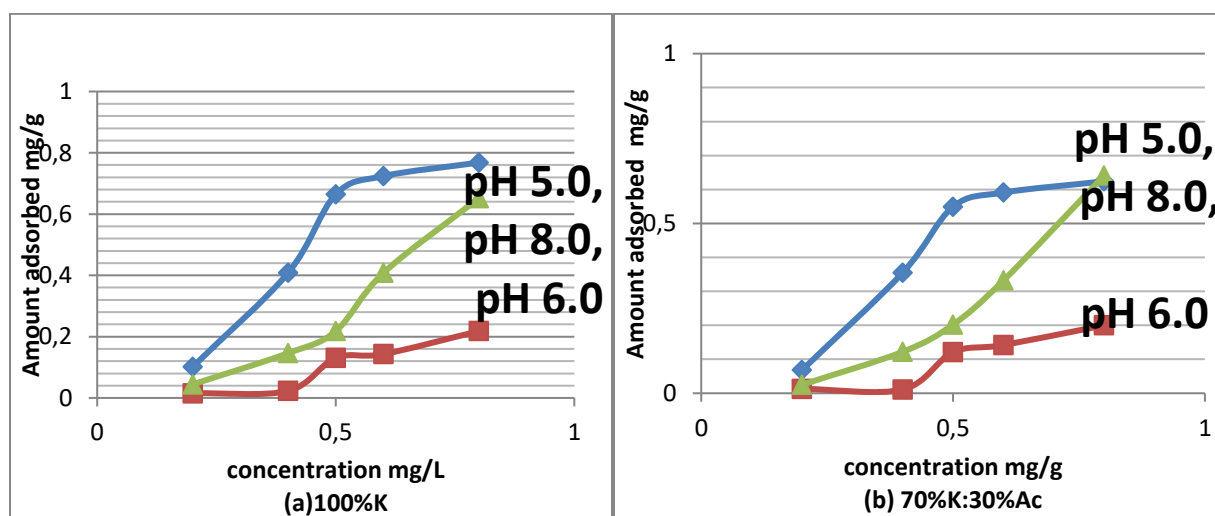


Figure 1. Possible hydrogen bonding patterns involving (a) the N-H moiety and (b) the Cl atom in atrazine fragments and OH-group in kaolin/alginate fragments in CRs.



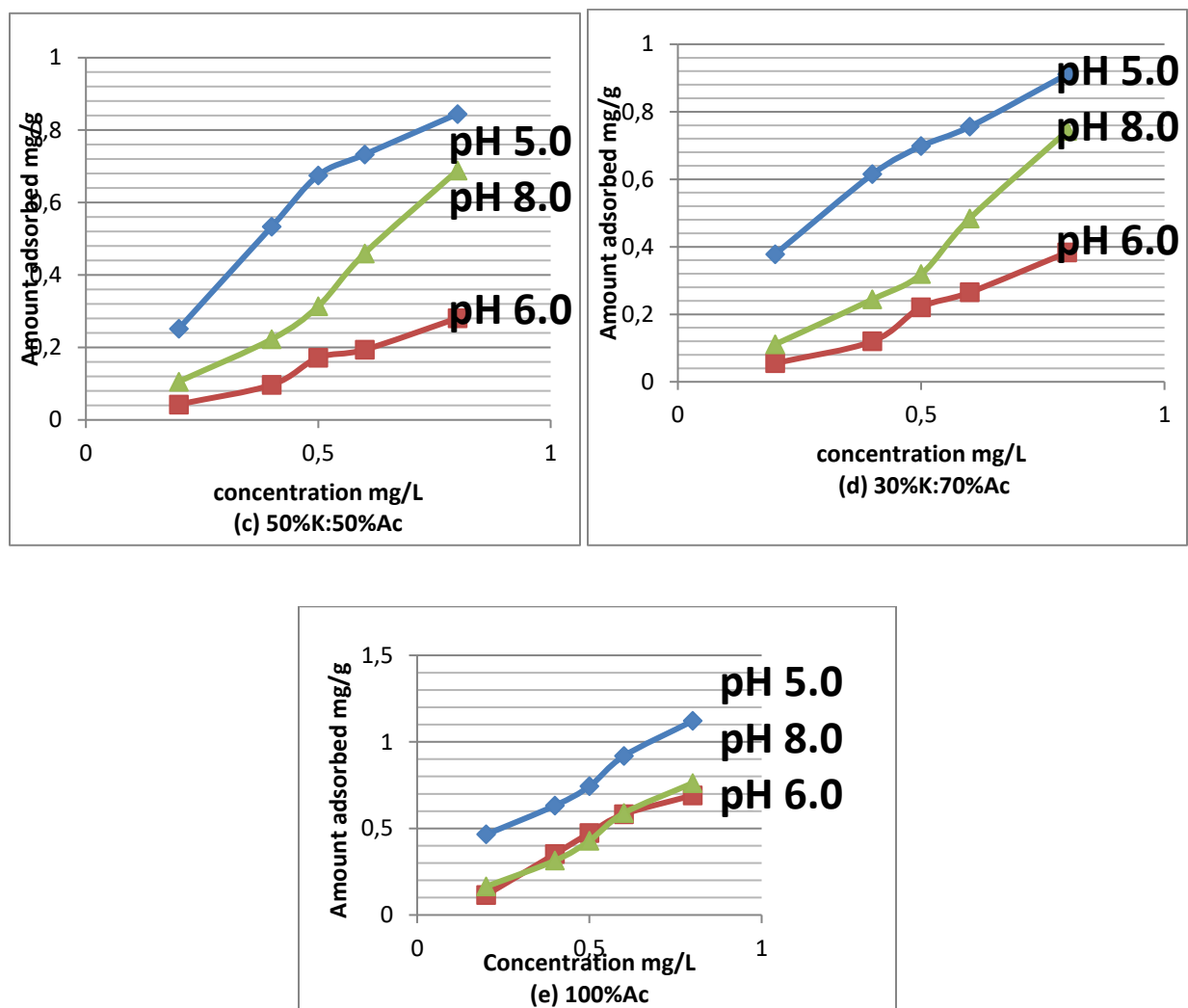


Figure 2. Graphs depicting pH effects on atrazine adsorption onto the different surfaces of (a) 100%K (b)70%K:30%Ac (c) 50%K:50%Ac (d) 30%K:70%Ac (e) 100%Ac.

Table 1. Rate data for the adsorption of atrazine on different surfaces at room temperature.

	K100	KC7030	KC5050	KC3070	C100
$k_1(s^{-1})$	9.0×10^{-2}	8.1×10^{-2}	8.6×10^{-2}	7.3×10^{-2}	7.7×10^{-2}
$t_{1/2}/\text{day}$	7.70	8.56	8.06	9.49	9.00
R^2	0.999	0.956	0.994	0.916	0.904

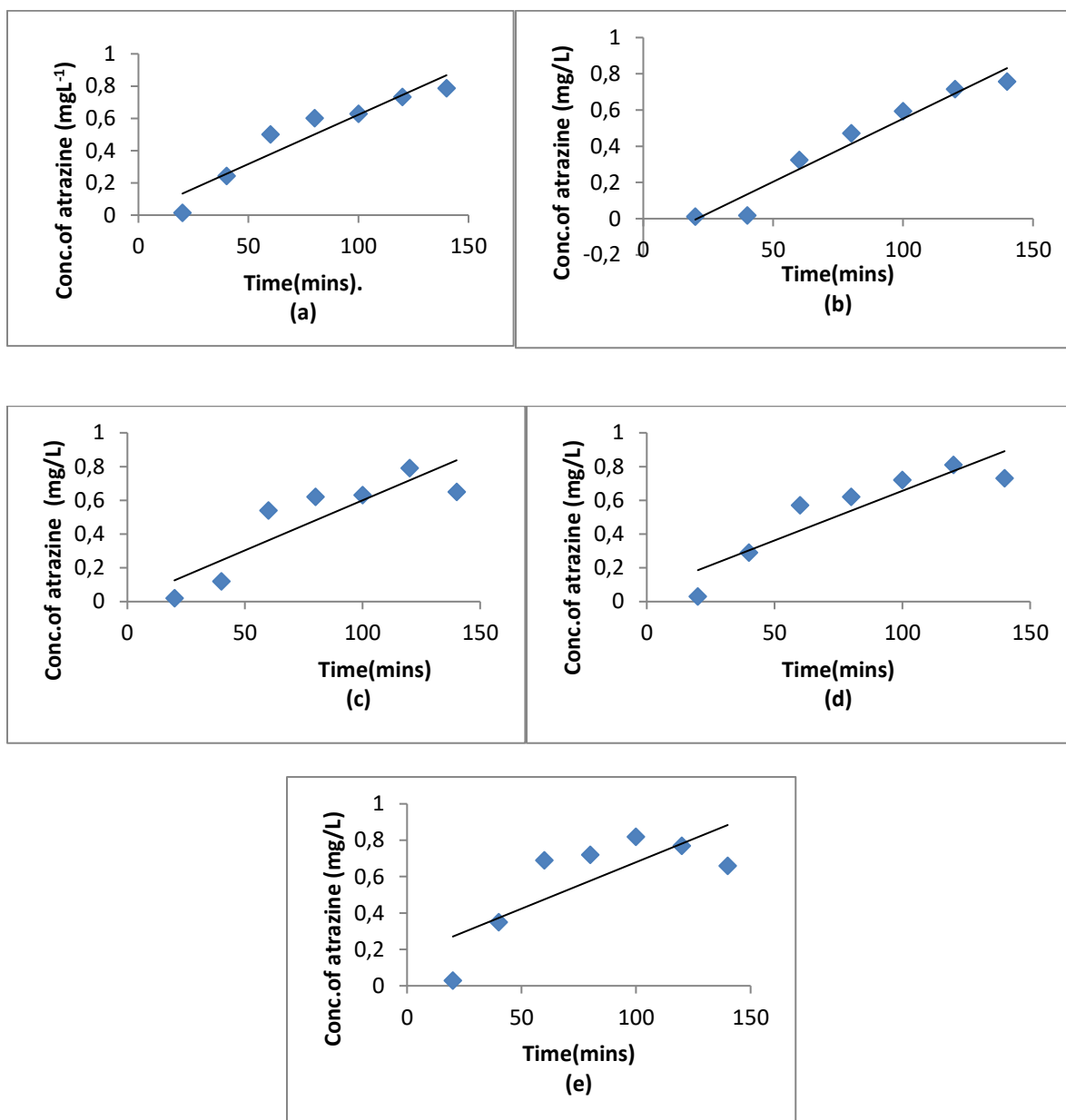


Figure 3. Zero-order kinetic plots for the adsorption of atrazine at pH 5 on (a) K100 (b) KC7030 (c) KC5050 (d) KC3070 (e) C100.

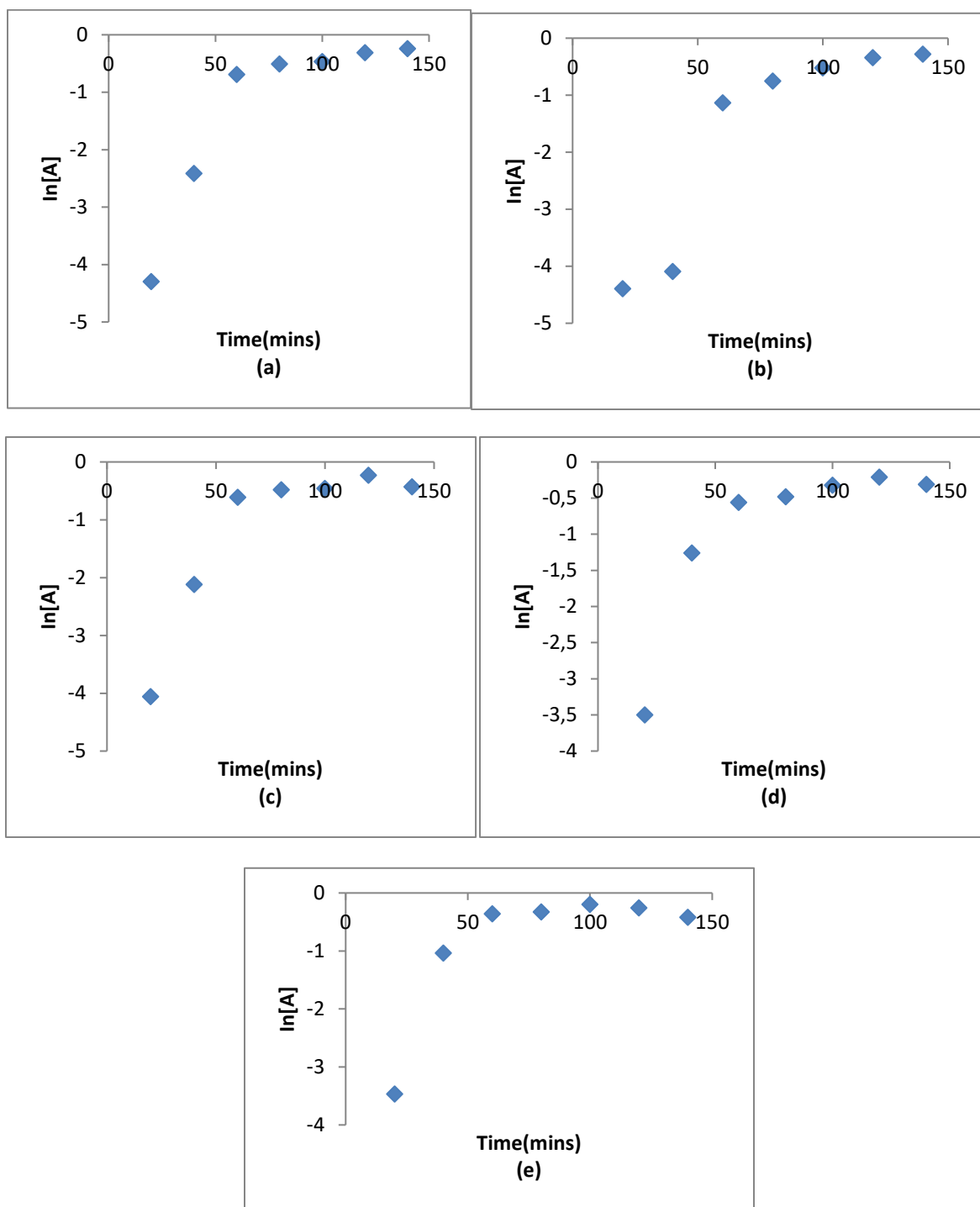


Figure 4. First order kinetic plots for the adsorption of atrazine at pH 5 on (a) K100 (b) KC7030 (c) KC5050 (d) KC3070 (e) C100.

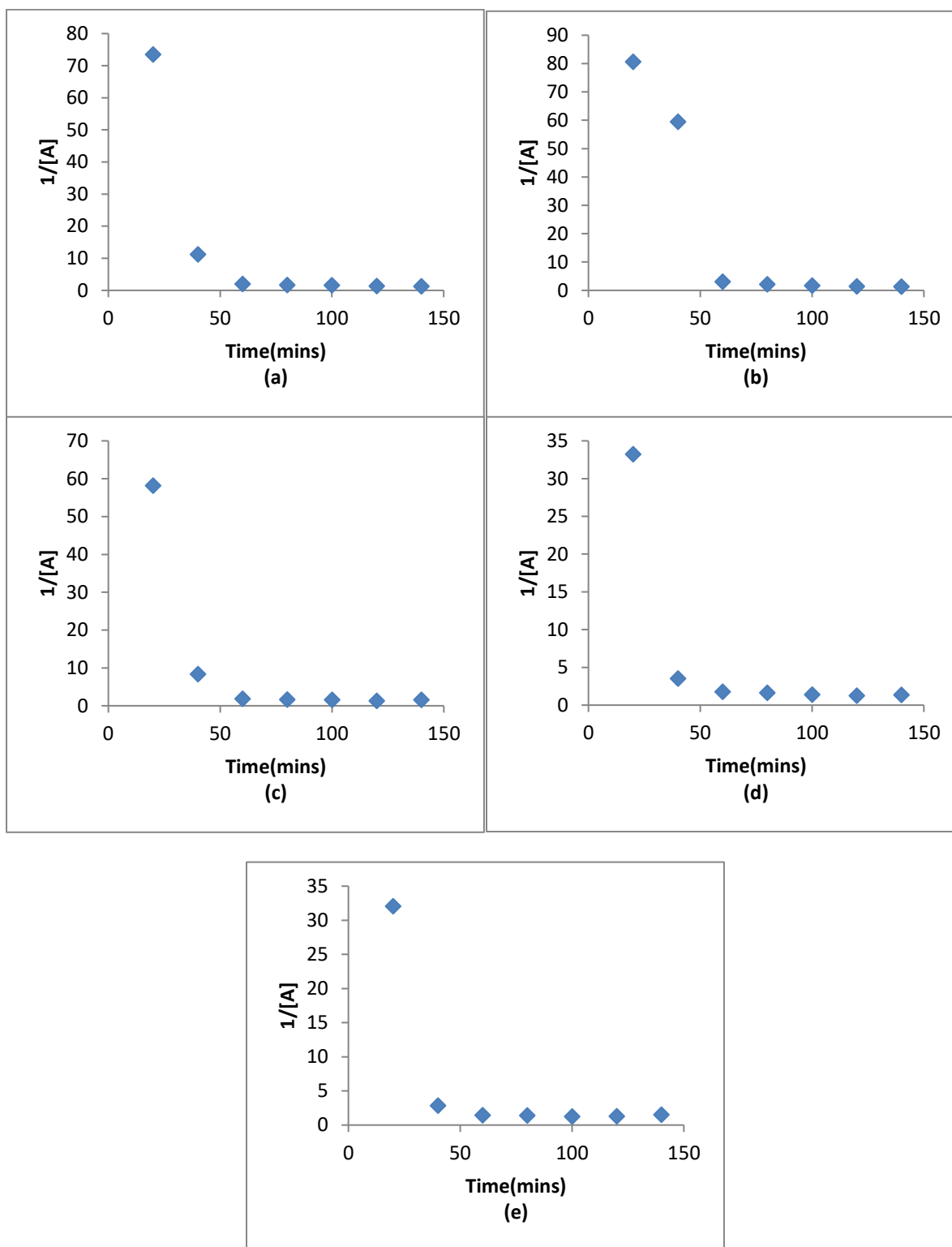


Figure 5. Second order kinetic plots for the adsorption of atrazine at pH 5 on (a) K100 (b) KC7030 (c) KC5050 (d) KC3070 (e) C100.

Table 2. Zero-order rate constants for the desorption of atrazine into water at room temperature from different surfaces, obtained by assuming zero-order behaviour.

	K100	KC7030	KC5050	KC3070	C100
$k_0(Ms^{-1})$	9.0×10^{-4}	8.0×10^{-4}	8.0×10^{-4}	8.0×10^{-4}	3.0×10^{-4}
$t_{1/2}/\text{day}$	12.94	29.75	35.63	35.44	48.33
R^2	0.936	0.913	0.940	0.903	0.972

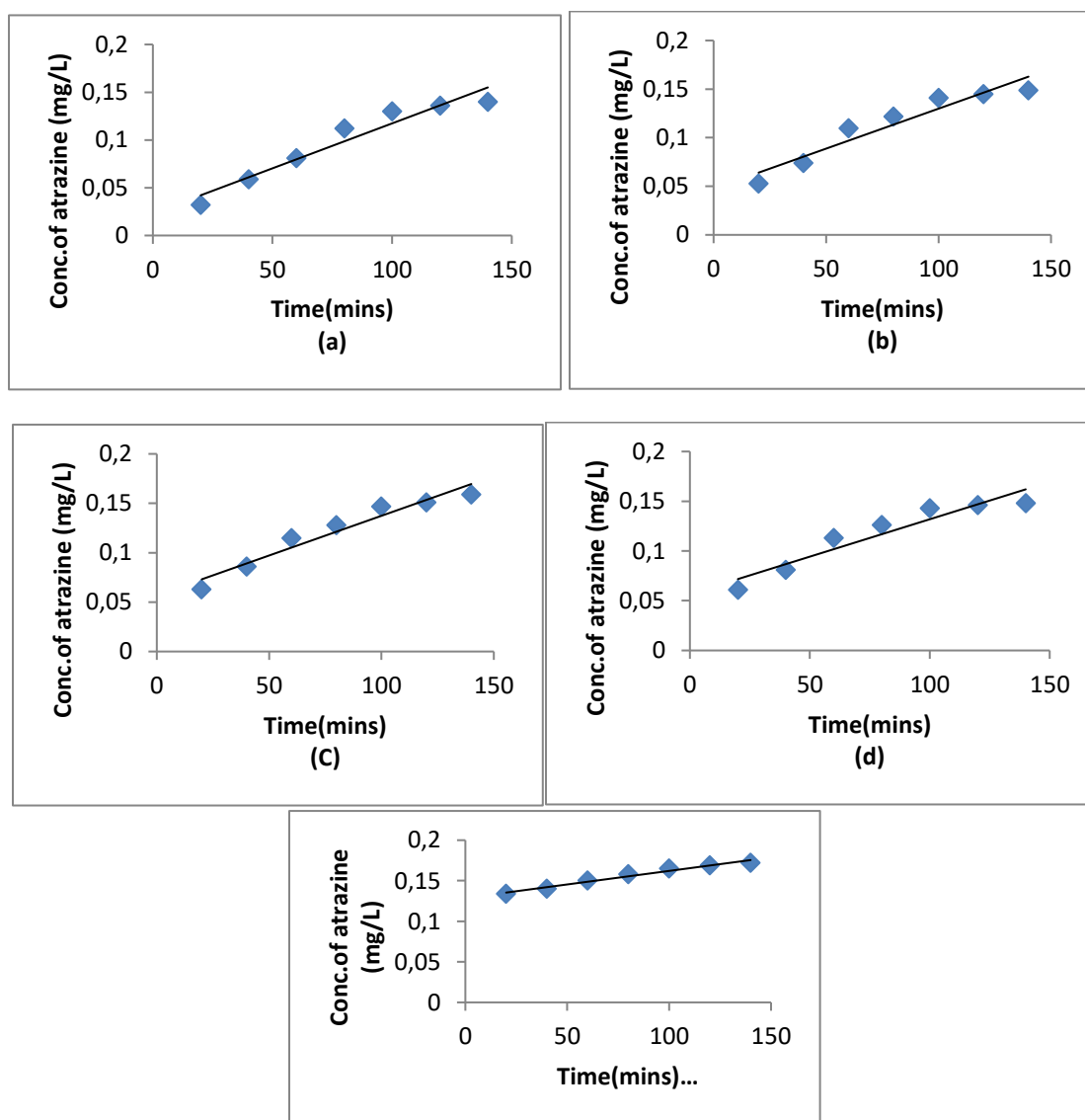
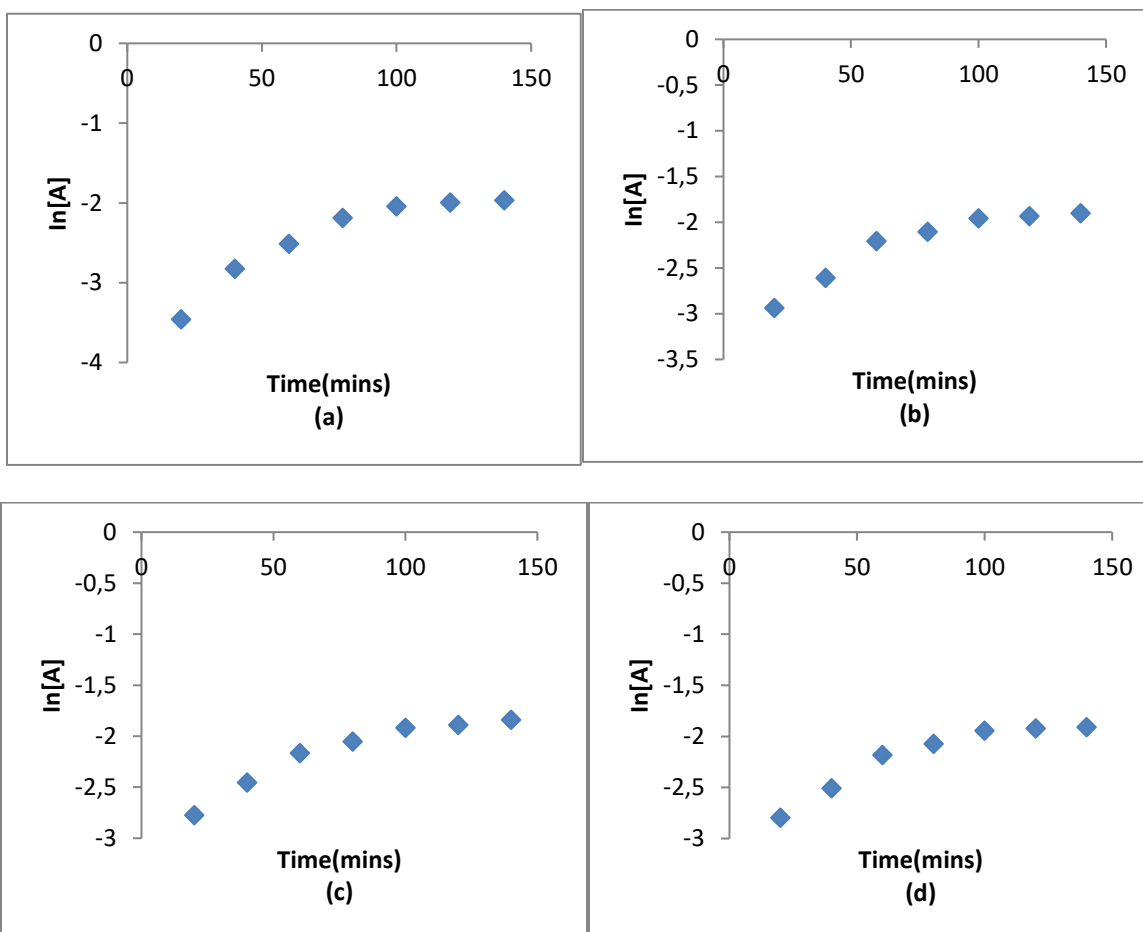


Figure 6. Zero-order plots of the amount released vs. time for the desorption of atrazine in water at pH 5 from (a) K100(b) KC7030 (c) KC5050 (d)KC3070 (e) C100.

Table 3. First-order rate constants for the desorption of atrazine into water at room temperature from different surfaces, obtained by assuming first-order behaviour.

	K100	KC7030	KC5050	KC3070	C100
$k_1(s^{-1})$	2.0×10^{-2}	1.8×10^{-2}	1.5×10^{-2}	1.5×10^{-2}	2.0×10^{-2}
$t_{1/2}/\text{day}$	34.65	38.50	46.20	46.20	34.65
R^2	0.988	0.998	0.998	0.998	0.989



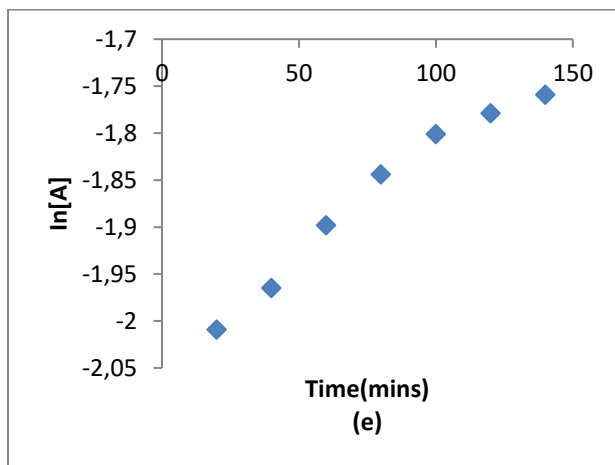
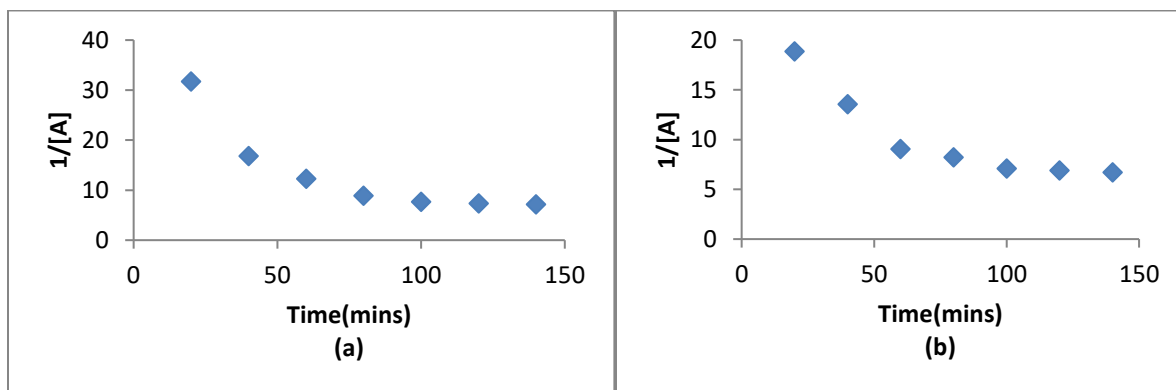


Figure 7. First-order plots of the amount of atrazine released vs. time for the desorption of atrazine in water at pH 5 from (a) K100 (b) KC7030 (c) KC5050 (d) KC3070 (e) C100.

Table 4. Second-order rate constants for the desorption of atrazine into water at room temperature from different surfaces, obtained by assuming second-order behaviour.

	K100	KC7030	KC5050	KC3070	C100
$k_2(M^{-1} s^{-1})$	4.86×10^{-1}	2.45×10^{-1}	2.91×10^{-1}	1.87×10^{-1}	1.9×10^{-2}
$t_{1/2}/\text{day}$	0.052	0.173	0.225	0.266	6.679
R^2	0.913	0.997	0.842	0.997	0.988



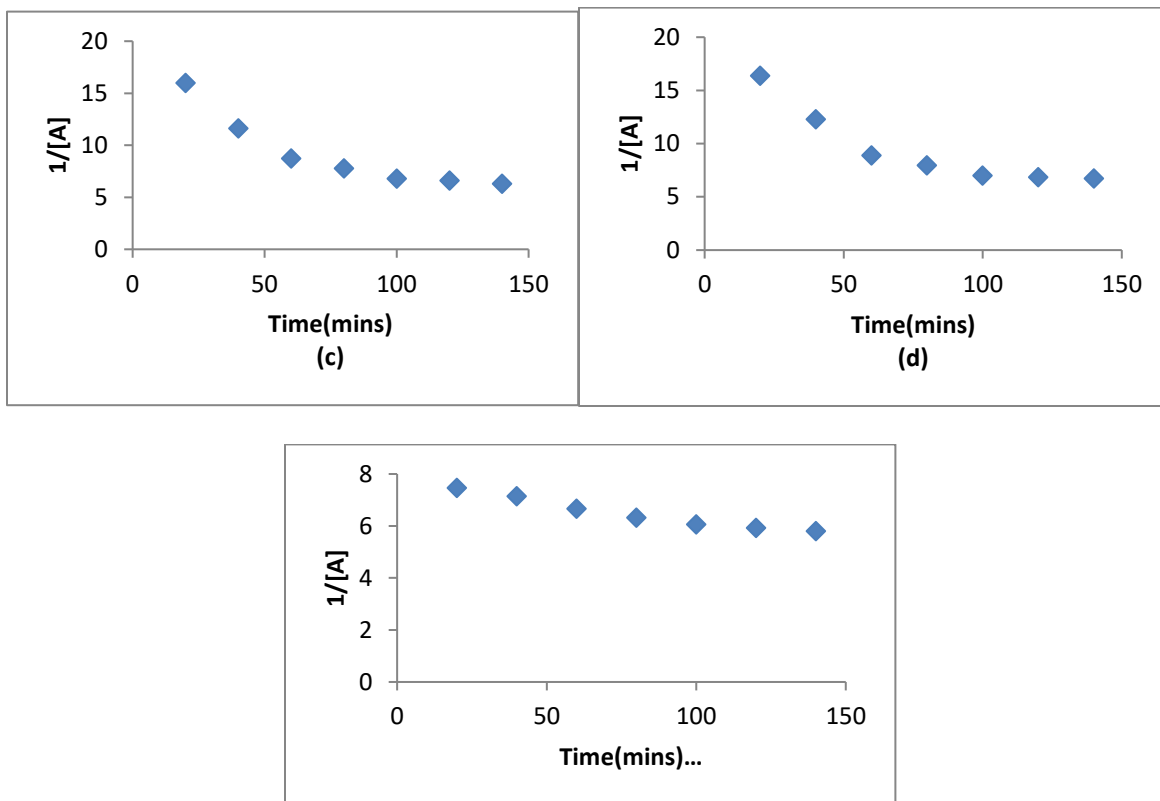


Figure 8. Second-order plots of the amount of atrazine released vs. time) for the desorption of atrazine in water at pH 5 from (a) K100 (b) KC7030 (c) KC5050 (d) KC3070 (e) C100.

Table 5. Rate and equilibrium constants for adsorption and desorption processes.

	K100	KC7030	KC5050	KC3070	C100	Total	Ave.
$k_{ads} (s^{-1})$	0.0900	0.0820	0.0860	0.0740	0.0780	0.4100	0.0820
$k_{des} (M^1s^{-1})$	0.0009	0.0008	0.0008	0.0008	0.0003	0.0036	0.0007
$k_{des} (s^{-1})$	0.0200	0.0180	0.0150	0.0150	0.0200	0.0880	0.0176
$k_{des} (M^{-1}s^{-1})$	0.4860	0.2450	0.2910	0.1860	0.1960	1.4040	0.2810

4. DISCUSSION

Effect of pH

The influence of pH on the charge state of the adsorbent surface makes it the main factor affecting the sorption processes. In terms of the effect of pH on atrazine adsorption, it was found that the extent of adsorption on all the surfaces was essentially the same at the different pHs investigated, such that adsorption at pH 5 ~ adsorption at pH 6 ~ adsorption at pH 8 as depicted in figure 2. Although Qiu *et al.*, (2015) have observed that acidic conditions are more favourable for atrazine adsorption because of the existence of charged (protonated) atrazine molecules, as shown in Scheme 1, at the lowest pH investigated in this study, i.e., pH 5, the proportion of protonated atrazine will be extremely small, since pK_a of atrazine = 1.7 (Qiu *et al.*, 2015).

In agreement with the finding above, the pesticide atrazine has been found to exist as a neutral molecule in the natural environment (pH ~ 5 - 8) (Colombini *et al.*, 1998, Jamil *et al.*, 2011).

Although several interactions, as discussed below, would conceivably be responsible for the adsorption of atrazine on different surfaces, hydrogen bonding is by far the more significant interaction at low pH (Welhouse and Bleam, 1993; Kovaivos *et al.*, 2006). Many interactions, such as electrostatic interactions (Salvestrini *et al.*, 2010), hydrophobic effects and van der Waals forces (Tang *et al.*, 2012) or hydrogen bonding (Kulikova and Perminova, 2002), have been reported to be involved in atrazine adsorption on various adsorbents. In the present study, the adsorption processes were studied in solutions of pH 5-8 (Ayadinuno E.O. *et al.*, 2026). Under these conditions, atrazine is adsorbed on the carbon surface as an uncharged molecule, and as a result, electrostatic interactions of the type involving charged species are not likely to play any role in adsorption from aqueous solutions. Rather, by a process of elimination, it can be inferred that in the pH range of the study, adsorption of atrazine on the surfaces studied is most likely to involve Van der Waals, hydrophobic, and similar non-bonding interactions (Schneider, 2003). Weak hydrogen bonding of the nature shown in Figures 1 (a) and (b) may also occur between the hydroxyl groups that abound in kaolin and the alginate used in the CR formulations and the N-H moiety or the Cl atom in atrazine. The aromatic ring of atrazine acting as a hydrogen bond acceptor to give weak H-bonds of $\sim 3 \text{ kcal mol}^{-1}$ is not a far-fetched idea (Levitt and Perutz, 1988).

Sorption Kinetics

Adsorption Kinetics

The kinetic behavior of the adsorption of atrazine on activated charcoal, kaolin, and activated charcoal-kaolin mixtures as adsorbents at pH 5 has been studied. Most studies reported in the literature as precursors of this investigation were studied at pH 5. This pH was chosen to enable cross-system comparison at the same pH. Data obtained from the adsorption kinetics were subjected to zero-order, first-order, and second-order plots in order to obtain a best fit model for the adsorption process. Equations 3, 4 and 5 represent the zero-order, first-order, and second-order rate expressions, respectively.

$$[A] = [A_0] - k_0t \quad 3$$

$$\ln[A] = \ln[A]_0 - k_1t \quad 4$$

$$1/[A] = 1/[A]_0 + k_2t \quad 5$$

Adsorption data were subjected to different plots in order to determine the kinetic order that best describes the adsorption process at pH 5. To obtain zero-order plots shown in Figure 3, the concentration of atrazine, $[A]$ was plotted against time according to equation 3. To obtain first-order plots, the adsorption data were plotted according to equation 4, which demands a plot of $\ln [A]$ versus time. The first-order plots are presented in Figure 4. Finally, treatment of the data in Table A6 according to equation 5 for second-order reactions, by plotting $\frac{1}{[A]}$ against time, resulted in the plots presented in Figure 5.

The outcomes of the plots in Figure 3 –5 are now discussed, starting from the second-order plots in Figure 5. The second-order rate expression of equation 5 predicts a straight line from the plot of $\frac{1}{[A]}$ against time. It is clear from Figure 5 that equation 5 is not obeyed by atrazine adsorption on the surfaces studied at pH 5. This leaves Figures 3 and 4 for zero-order and first-order behaviour respectively, for further consideration.

The plots for zero-order behaviour mostly do not conform to equation 3 both by visual inspection and from the value of R^2 obtained from the different plots. Although the plausibility of the system manifesting zero-order kinetics with significant error is admissible, such consideration is inferior to the argument for first-order behaviour which the plots of $\ln[A]$ versus time for first-order behaviour. The plots shown in Figure 4 clearly manifest saturation kinetics on all the surfaces. Saturation kinetics which show an initial linear response of to time but which attains a plateau is consistent with the Langmuir isotherm in which an equilibrium saturation point is reached once available sites are occupied by a unimolecular layer of the adsorbate (Foo and Hameed, 2010).

The first-order rate constants, k_1 , obtained from plots, of the linear portions of the graphs presented in Figure 4, along with the R^2 values for the plots are presented in Table 1. The k_1 value does not vary in any systematic way. Given the magnitude of error associated with these measurements, implicit in the R^2 values, it can be argued that these values of k_1 do not vary substantially amongst themselves as there is only a difference of 23% between the highest and lowest values. The significant result here is that the composite matrices do not promote adsorption better than the pure surfaces. It is, however, noteworthy from the plots that on all the surfaces investigated, equilibrium is established around 50 minutes.

The plots for second-order kinetics on all the surfaces investigated at pH 5 according to equation 5 are assembled in Figure 5. Although the plots give the impression of second-order behaviour which precedes attainment of equilibrium, the paucity of points in the initial phase of the plot does not allow a discussion of this kinetic behaviour to be pursued further.

Having considered the viability of the different rate equations for zero-order, first-order, and second-order behaviour in modeling the kinetic data obtained for adsorption on different surfaces, it is concluded that the saturation kinetics obtained by treatment of the rate data as first-order behaviour is best suited to the Langmuir isotherm, which the adsorption data conform to. First-order sorption behaviour was also reported by Donald and Shahamat (2011) in atrazine in mineral soil: chemical species and catalysed hydrolysis, with sorption rate constants in the range of 0.1925 - 0.0009 day⁻¹ while sorption half-life ranged from 3.6 to 735 days.

The first-order constants and half-lives obtained in this work are of similar order of magnitude as that reported in the literature. The k_1 obtained is in the range of 0.077 to 0.09 with the $t_{1/2}$ ranging from 7.70 to 9.00 days. For Protzman *et al.* (1999) and Armstrong *et al.* (1967), the half-lives of atrazine vary greatly from 45 days to 3-5 years, depending on environmental conditions. The values of k_1 and $t_{1/2}$ obtained in this work done in aqueous environment in the laboratory, do not fall within the range reported by these workers.

Desorption Kinetics

Desorption kinetics of atrazine from the different surfaces were determined by measuring the decrease in the concentration of atrazine with time, following the attainment of equilibrium in the sorption kinetics experiments. The kinetic data so obtained were plotted to obtain Figure 6 – 8 according to equation 3-5 for zero-order, first-order, and second-order kinetics.

Analysis of the kinetic data according to zero-order behaviour gave the plots presented as Figure 6. The parameters obtained from these plots are summarized in Table 2. The values of R^2 obtained for desorption from the surfaces are ≥ 0.903 , suggesting about 90% linearity of the plots. These values make reaction via zero-order kinetics a plausible possibility. Though zero-order kinetic behaviour are not very common in the literature, Arica *et al.* (1997) reported that the use of high molecular weight carboxymethylcellulose microcapsules (CMC) in the controlled release formulation of aldicarb, a drug, follows zero-order kinetic.

Treatment of the kinetic data by assuming first-order behaviour according to equation 4 gives the plots in Figure 7. The resulting first-order plots for desorption from the different surfaces show saturation behaviour in which there is an initial linear portion of the plot which attains a plateau, signifying the attainment of equilibrium. First-order rate constants obtained from the linear portion of the plots, along with the calculated $t_{1/2}$ values and R^2 values, are given in Table 3.

The first-order rate constants, k_1 obtained in this work fall within the range 0.017 to 0.052 with the half-life, $t_{1/2}$ ranging from 34.65 to 46.20 days. These values are in accord with the work of Jaikraw *et al.* (2017) in which the desorption data fitted the first-order model with half-life ranging from 19.2 to 46.9 days for atrazine (46.9 at 5°C, 49.7 at 20°C and 19.2 at 35°C) with the rate constants been in the range of 0.036 to 0.015. Also, Al-Wabel *et al.* (2010), measured the degradation rate for atrazine as 0.0102/day with the half-life accounted as 68.1 days. Vryzas *et al.* (2012) reported that the half-life of atrazine ranges from 5-18 days. Another study by Gaynor *et al.* (1998) stated that the half-life of atrazine ranged from 31 to 66 days. The low half-life values reported in the literature (Barriuso and Houot, 1996; Vanderheyden *et al.*, 1997; Singh *et al.*, 2009; Yassir *et al.*, 1999) were related to (i) high soil pH which support high bacterial biomass, (2) soil exposed to repeated applications of pesticides, and (3) specific management practices.

In this work, pure kaolin and activated charcoal have similar rate constants with half-life of 34.65 days. The rate constants for the composites are a bit lower than that of the pure surfaces, with half-life ranging from 38.5 to 46.20 days. KC5050 and KC3070 both have the highest half-life of all the matrices investigated, with a value of 46.20 days. This means that both surfaces have the ability to hold on to atrazine longer than others; hence, these are the most likely matrices for atrazine slow-release formulations (SRFs).

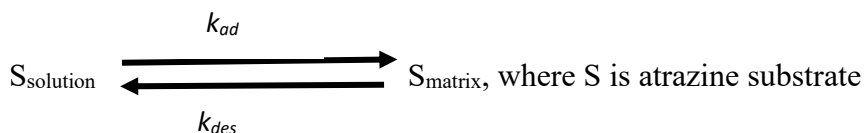
To model kinetic data according to second-order expression of equation 5, $\frac{1}{[A]}$ is plotted against time to obtain the plots in Fig. 8 for the different surfaces investigated. These plots are basically biphasic in shapes: there is an initial rapid linear portion which gradually flattens out, consistent with an equilibrium process. The linear portion is utilized to calculate second-order rate constants, which are displayed in Table 4, along with the R^2 values obtained.

From Table 4, pure activated charcoal has the lowest k_2 value and hence the highest $t_{1/2}$ of all the surfaces investigated, while pure kaolin has the highest k_2 and the lowest $t_{1/2}$ values of the surfaces. The k_2 and $t_{1/2}$ of the composites fall in between the two surfaces, with the order ranging from 0.052-6.679. In the work of Nkwaju *et al.*, (2016) involving the influence of modification of the activated charcoal on adsorption of atrazine, second-order model was observed, with the surfaces investigated having $t_{1/2}$ of 0.12 for pure activated charcoal (PAC), 0.27 for activated charcoal treated with nitric acid (AC-HNO₃) and 0.08 for silver treated AC (AC-Ag). This shows that the values obtained in our work corresponded with that reported in the literature for the activated charcoal surfaces. The $t_{1/2}$ value for the pure kaolin and activated charcoal surfaces implies that activated charcoal can hold on to atrazine much longer than pure kaolin surface and the composites; hence, it is likely to be a better matrix for atrazine SRFs.

The kinetic results are unable to distinguish between zero-order, first-order, and second-order desorption. This is not unusual, as this lack of discrimination has been observed in the sorption kinetics of a number of adsorbates on different surfaces (Achintya, *et al.*, 2009; Liwang and Selim, 2005)

Kinetically Determined Equilibrium Constants

The sorption equilibrium can be written as:



The forward process is adsorption, with the rate constant k_{ad} . The backward process is desorption, with rate constant k_{des} . The equilibrium constant, as determined from the kinetic constants, is shown in equation 6

$$K_{ads} = \frac{k_{ads}}{k_{des}} \quad 6$$

If the equilibrium is viewed from the backward direction, then the equilibrium constant K_{des} is defined as in equation 7, from which the relationship in equation 8 is obtained.

$$K_{des} = \frac{k_{des}}{k_{ads}} \quad 7$$

Which is the same as
$$K_{des} = \frac{1}{K_{ads}} \quad 8$$

The values of $k_{ads}(s^{-1})$ show that the rate of adsorption is, to a first approximation, independent of the surface such that $k_{ads} = 0.0820 \pm 0.003 s^{-1}$. Also, the values of $k_{des}(s^{-1})$ are small and could conceivably incorporate a large measurement error. One may therefore assume that the $k_{des}(s^{-1})$ values in Table 5 are also independent of the surfaces, so that $k_{des} = 0.0176 \pm 0.003 s^{-1}$. This gives a K_{des} of 4.659. This positive value is in the range of the K_L values measured for the different surfaces according to the Langmuir isotherm. Assuming second-order desorption kinetics gives a value of $k_{des} = 0.281$, this gives a K_{des} of $\frac{0.082}{0.281} = 0.292 (gcm^{-1})$

The value of K_L obtained by assuming second-order desorption is significantly lower than that obtained experimentally. It is seen that the kinetic model that fits the Langmuir isotherm is one in which the adsorption-desorption equilibrium can be described in kinetic terms in which the adsorption process is first-order in the forward direction and first-order in the reverse direction.

5. CONCLUSION

The kinetics of the sorption process showed that first-order behaviour better describes the rate processes for adsorption on all the surfaces investigated. For desorption, no clear distinction between first-order and second-order behaviour was established. However, determination of the adsorption capacity, K_L , of the systems investigated by kinetic procedure ($K_L = \frac{k_{ads}}{k_{des}}$) showed that a K_L value, which is the same range as that obtained thermodynamically, is obtained when first-order behaviour is assumed for the reverse process.

Acknowledgement

The author acknowledged Emeritus Professor Ikenna Onyido, FAS, who solely supervised this work, and the National Agency for Food and Drug Administration and Control (NAFDAC) for giving me the opportunity to use their regional laboratory at Agulu, Anambra State, Nigeria.

References

- [1] Achintya, N.B., Jay, M.T. and Bret, J.C. (2009): Remediation of Alachlor and Atrazine Contaminated water with zero-valent iron nanoparticles. J.Environ.Sci.and Health, part B, 44:518-524.
- [2] Al-Wabel, M.I., Abdel-Nasser, G., Al-Turki, A.M and El-Saeid, M.H. (2010): Behaviour of Atrazine and Malathion Pesticides in Soil: Sorption and Degradation processes. J.Applied Sci., 10: 1740-1747.
- [3] Armstrong, D.; Chesters, G.; Harris, R. (1968): Adsorption catalyzed chemical hydrolysis of atrazine., Environ. Sci. Technol., 31: 61-66.

- [4] Arica, M.Y., Mustafa, Y., Mustafa, L., Fatma, N.K and Vasif, H. (1997): Controlled Release of Aldicarb from carboxymethylcellulose Microcapsules. *J. Chem.* 21:100-104.
- [5] Ayadinuno Emmanuel Onyenweife, and Maryjane Ogechi Ejiako (2026): Adsorption-desorption characteristics of atrazine on activated charcoal and kaolin composite matrices and the In vitro performance of their CRFs, *WSN 211 (2026) 311-328* EISSN 2392-2192, <http://doi.org/10.65770/SOSY3277>
- [6] Barriuso, E., Houot, S. (1996): Rapid Mineralization of the S-triazine ring of Atrazine in Soils in Relation to Soil Management. *Soil Biology and Biochemistry*, 28(10): 1341-1348.
- [7] Cleuciane Tillvitz do Nascimento, Melissa Gurgel Adeodato Vieira b, Fabiano Bisinella Scheufele c, Fernando Palú a, Edson Antonio da Silva a, Carlos Eduardo Borba (2022): Adsorption of atrazine from aqueous systems on chemically activated biochar produced from corn straw. *Journal of Environmental Chemical Engineering* Volume 10, Issue 1, Feb., 107039 <https://doi.org/10.1016/j.jece.2021.107039>
- [8] Colombini, M.P., Fuoco, R., Giannarelli, S., and Pospíšil, L.T. (1998): Protonation and Degradation Reactions of S-Triazine Herbicides. *Microchemical Journal*, 59: 239-245.
- [9] Cruz-Guzmn, M., Celis, R., Hermosin, M.C., Koskinen, W.C., Cornejo J. (2005) Adsorption of pesticides from water by fuctionalized organobentonites, *J. Agric. Food Chem.*, 53(19): 7502.
- [10] Donald, G. and Shahamat, U.K (2011): Atrazine in Mineral Soil; Chemical Species and Catalysed Hydrolysis. *Canadian Journal of Chemistry*, 70(6): 1597-1603.
- [11] Foo, K.Y, Hameed, B.H (2010): Insights into the modeling of adsorption isotherm systems; *Chemical Engineering Journal*, 156(91): 2-10, ISBN 1385-8947.
- [12] Gaynor, J.D., Mactawish, D.C and Labaj, A.B. (1998): Atrazine and Metolachlor Residues in Brookston Cl Following Conventional and Convservation Tillage Culture. *Chemosphere*, 36(15): 3199-3210.
- [13] Jaikraew, P., Farag, M.M., Boulange, J., Watanabe, H. (2017): Degradation and Adsorption Kinetics of Atrazine and Metolachlor in Andisol Soil. *Hellenic Plant Protection journal*, 10(1): 1-14.
- [14] *Jamil, T.S., T. A. Gad-Allah, H.S. Ibrahim, T.S. Saleh (2011): Adsorption and isothermal models of atrazine by zeolite prepared from Egyptian kaolin. Solid State Sciences 13 (1): 198-203.*
- [15] Javier M. Gonzalez a, Lynnette R. Murphy b c, Chad J. Penn a, Veera M. Boddu d, Laura L. Sanders (2020); Atrazine removal from water by activated charcoal cloths, *International Soil and Water Conservation Research*, Volume 8, Issue 2, June, Pages 205-212, <https://doi.org/10.1016/j.iswcr.2020.03.002>
- [16] Jones, T.W., W.M.Kemp, J.C.Stevenson and J.C. Means (1982): Degredation of atrazine in estuarine water/sediment systems in soils, *J. Environ. Qual.*, 11: 632-638.
- [17] Kovaiosi, L.D, Paraskeva, C.A and Koutsoukos, P. G. (2011): Adsorption of atrazine from aqueous solution on humic acid and silica in *J. Colloid Interface Sci.*, Vol. 356: 277-285.
- [18] Levitt, M.and Perutz, M. F. (1988): Aromatic rings can act as hydrogen bond acceptors. *Journal of Molecular Biology*, 201: 751-754.

- [19] Liwang, M. and Selim, H.M. (2005): Predicting Pesticide Transport in Mulch-Amended Soils: A Two component Model. *Soil Sci. Soc. Am. J.* 69: 318-327.
- [20] Nkwaju, Y. R., Kouotou, D., Bacaoui, A., Dammi, D. E., Gaelle, Y.A. and Ketcha, J. M. (2016): Influence of Modification of the Activated Carbon on Adsorption of Atrazine: Equilibrium Study and Kinetics. *Intl J.Engr.Sci and Research*, 5(9): 128-138.
- [21] Qiu, J., Wang, G., Bao, Y., Zeng, D. Z. and Chen, Y. (2015): Effect of oxidative modification of coal tar Pitch-Based mesoporous activated carbon on the adsorption of Benzothiophene and dibenzothiophene. *Fuel process technology*, 129: 85-90
- [22] Prasanta Majee & P Hari Prasad Reddy (2023): Sorption behaviour of atrazine on agricultural soils of different characteristics: equilibrium and kinetics studies: Volume 25, pages 3407–3417, (2023), *J.of Clean Technologies and Environmental Policy*
- [23] Protzman R. S., Lee P. H., Ong S. K., Moorman T.B. (1999): Treatment of formulated atrazine rinsate by agrobacterium radiobacter strain in a sequencing batch biofilm reactor. 33: 1399-1404.
- [24] Schneider, P. R. (2003): Metal free organocatalysis through explicit hydrogen bonding interaction, *Chemical Society Reviews*, 32: 289-296.
- [25] Singh, B., Sharma, D, K., Kumar, R., and Gupta, A. (2009): Controlled release of the fungicide thiram from starch –alginate clay-based formulation, *Applied Clay Sci.* 45: 76-82.
- [26] Sun Jing, Ma Xiu Lan, Wang Wen, Zhang Jing, Zhang Hao and Wang Yu Jun (2020): Adsorption characteristics of atrazine on different soils in the presence of Cd (II); *Adsorption Science & Technology* 2020, Vol. 38(7–8) 225–239 DOI: 10.1177/0263617420928845 journals.sagepub.com/home/adt
- [27] Tang, W.W., Zeng, G.M., Gong, J. L., Liu, Y., Wang, X. Y., Liu, Y.-Y., Liu, Z.F., Chen, L., Zhang, X.-R. and Tu, D.-Z. (2012): Simultaneous Adsorption of Atrazine and Cu (II) from Wastewater by Magnetic Multi-Walled Carbon Nanotube. *Chemical Engineering Journal*: 211-212, 470-478.
- [28] Vanderheyden, V., Debongnie, P. and Pussemier, L. (1997): Accelerated Degradation and Mineralization of Atrazine in Surface and Subsurface Soil Materials. *Pesticide Science*, 49(3): 237-242.
- [29] Vryzas, Z., Papadaki, E.N. and Papadopoulou, M. E. (2012): Leaching of Br⁻, Metolachlor, Alachlor, atrazine, Deethylatrazine and Deisopropylatrazine in dayey vadoze zone: A field scale experiment in north-east Greece. *Water Research*, 46(6): 1979-1989.
- [30] Yamil L. Salomón^a, Jordana Georgin^a, Dison S.P. Franco^b, Matias S. Netto^b, Daniel G.A. Piccilli^a, Edson Luiz Foletto^b, Diana Pinto^c, Marcos L.S. Oliveira^{c,d}, Guilherme L. Dotto (2022): Adsorption of atrazine herbicide from water by diospyros kaki fruit waste activated carbon; *Journal of Molecular Liquids*, Volume 347, 117990, <https://doi.org/10.1016/j.molliq.2021.117990>
- [31] Yassir, A., Lagacherie, B., Houot, S., Soulas, G. (1999): Microbial aspects of Atrazine Biodegradation in relation to History of Soil Treatment. *J.of Pesticide Sci.*, 55(8): 799-809.